A Method for MPPT Control While Searching for Parameters Corresponding to Weather Conditions for PV Generation Systems

Nobuyoshi Mutoh, *Senior Member, IEEE*, Masahiro Ohno, and Takayoshi Inoue

***Abstract*—This paper describes a method for maximum power point tracking (MPPT) control while searching for optimal parameters corresponding to weather conditions at that time. The conventional method has problems in that it is impossible to quickly acquire the generation power at the maximum power (MP) point in low solar radiation (irradiation) regions. It is found theoretically and experimentally that the maximum output power and the optimal current, which give this maximum, have a linear relation at a constant temperature. Furthermore, it is also shown that linearity exists between the short-circuit current and the optimal current. MPPT control rules are created based on the findings from solar arrays that can respond at high speeds to variations in irradiation. The proposed MPPT control method sets the output current track on the line that gives the relation between the MP and the optimal current so as to acquire the MP that can be generated at that time by dividing the power and current characteristics into two fields. The method is based on the generated power being a binary function of the output current. Considering the experimental fact that linearity is maintained only at low irradiation below half the maximum irradiation, the proportionality coefficient (voltage coefficient) is compensated for only in regions with more than half the rated optimal current, which correspond to the maximum irradiation. At high irradiation, the voltage coefficient needed to perform the proposed MPPT control is acquired through the hill-climbing method. The effectiveness of the proposed method is verified through experiments under various weather conditions.**

***Index Terms*—Current control, irradiation, maximum power point tracking (MPPT), photovoltaic (PV), PV power generation.**

I. Introduction

STUDIES on photovoltaic (PV) generation systems are actively being promoted in order to mitigate environmental issues such as the green house effect and air pollution. PV generation systems have two big problems, namely: 1) the efficiency of electric power generation is very low, especially under low radiation states, and 2) the amount of electric power generated by solar arrays is always changing with weather conditions, i.e., irradiation. Therefore, a maximum power point tracking (MPPT) control method to achieve maximum power (MP) output at real time becomes indispensable in PV generation systems. Thus, many MPPT controllers that are indispensable tools in PV generation systems have been proposed [1]–[15]. The "perturbation and observation" (P&O) method, which is well known as the "hill-climbing method," is widely applied in these controllers since the structure of PV generation systems becomes simple. The P&O method is also used in solar cars for racing, where miniaturization and lightweight are indispensable. MP point trackers have the P&O method embedded [1], [2] and are supplied from Beil and Brush [3], [4], etc., as racing kits. These kits are normally converted according to specifications of each solar car [1], [2]. However, various problems occur in the P&O method when acquiring the MP. For example, there are two kinds of the well-known algorithms to execute the P&O method. One is the algorithm [5], [6] that searches for the MP while checking the sign of the differential coefficient (dP/dI) of the power (P) with respect to the current (I) in the $P-I$ characteristics. The other is the algorithm [7] that searches for the MP while checking the sign of the differential coefficient (dP/dV) of the power (P) with respect to the voltage (V) in the $P-V$ characteristics. As oscillations always appear in the method, the power loss may be increased. Moreover, there is also a problem in the latter algorithm in that it becomes difficult to acquire the MP at lower irradiation since the peak appearing in the $P-V$ characteristics drops remarkably according to the reduction in irradiation. The "limit cycle method" is proposed [8] to reduce high frequency loss; it searches for the equilibrium point of the inverter output power while moving the current and voltage within the predetermined limits. Although oscillation with high frequencies may be reduced, it takes much time to acquire the MP and fluctuations of the power may be produced under steady states. Moreover, there is the "incremental conductance method," which is a technique to reduce the oscillation appearing in the ordinary P&O method. This technique searches for the MP while checking the sign of the incremental conductance (dI/dV) [9]. It is difficult to find out the MP in lower irradiation regions since this is the technique to search for the MP based on $P-V$ characteristics.

Moreover, there are "fuzzy and neural network methods" [10], [11] that focus on the nonlinear characteristics of solar arrays. Since it is necessary to create control rules that meet the output characteristics of the solar arrays, the methods lack versatility. In addition, it takes much time to acquire the MP immediately after extending or updating the solar arrays. The "DSP-controlled method" [12] performs the P&O algorithm at high speeds. Although the frequencies of oscillations are shifted

Manuscript received December 31, 2004; revised October 14, 2005. Abstract published on the Internet May 18, 2006.

N. Mutoh is with the Graduate School, Tokyo Metropolitan University, Tokyo 191-0065, Japan (e-mail: nmutoh@cc.tmit.ac.jp).

M. Ohno is with the Graduate School, Tokyo Metropolitan Institute of Technology, Tokyo 191-0065, Japan.

T. Inoue was with the Graduate School, Tokyo Metropolitan Institute of Technology, Tokyo 191-0065, Japan. He is now with Meidensha Corporation, Tokyo 100, Japan.

Digital Object Identifier 10.1109/TIE.2006.878328

to higher regions, it is difficult to reduce the power loss and noises as long as the ordinary P&O method is used. In order to solve these difficulties, the "integrated MPP control method" is proposed [13], which performs MPPT control for every solar panel that is divided into two or more panels. This has difficulty in securing a reliable power supply. These days, methods for avoiding the problems of the P&O method have been proposed [14], [15]. One of them is the "short-circuit current measurement method" [14] to perform MPPT control while a short-circuit current flows for measurements in the circuit. Although this method does not have oscillations like those appearing in the P&O method, the power loss may increase since the short-circuit current flows whenever MPPT control is performed. Furthermore, it becomes difficult to perform MPPT control in low irradiation regions because the short-circuit current decreases in accordance with irradiation. Another proposed method [15] searches for the intersection between the $P-I$ function and the line of the MP. Although oscillations are also generated by this technique, it is impossible to perform MPPT control over a wide range of irradiation since power becomes a binary function of the current. Accordingly, when using the $P-I$ characteristics, MPPT control rules that determine the optimal current reference by dividing the $P-I$ characteristics into two control fields are needed, as shown previously [16], [17]. Furthermore, the compensation for variations of the proportionality coefficient (voltage coefficient) between the MP and the optimal current that occurs due to the temperature change of solar panels should also be considered in these control rules.

In this paper, first, the linear relationship between the MP and the optimal current is clarified through theoretical analyses and experiments, and then control rules for executing MPPT control are constructed based on the analyzed results. Finally, the created control rules are used, and the effectiveness of the proposed MPPT control method is verified under various weather conditions.

II. Creation of Control Rules for Performing Precise and Quick MPPT Control

A. Relationship Between MP and Optimal Current

Here, first, the theoretical relationship between the maximum current and the optimal current is derived using the equivalent circuit shown in Fig. 1 [18]. The output current I of solar arrays is given by (1) using the symbols in Fig. 1, i.e.,

$$I = I_{\rm ph} - I_d - V_d/R_{\rm sh} \tag{1}$$

$$V_d = V + R_s I \tag{2}$$

$$I_d = I_o \left\{ \exp\left(\frac{qV_d}{nkT}\right) - 1 \right\} \tag{3}$$

here $I_{\rm ph}$ is the photocurrent (in amperes), I_0 is the reverse saturation current (in amperes), R_s is the series resistance (in ohms), $R_{\rm sh}$ is the parallel resistance (in ohms), n is the diode factor, q is the electron charge (in coulombs), k is Boltzmann's constant (in joules per kelvin), and T is the panel temperature (in kelvin). The components related to the diode are eliminated,

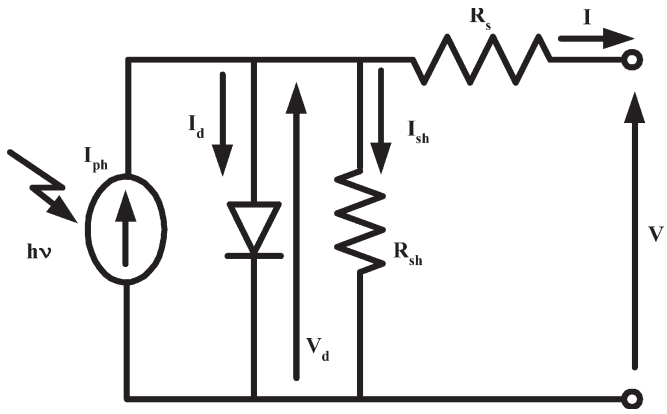

Fig. 1. Equivalent circuit for solar arrays.

and the output current I is expressed by

$$I = I_{\rm ph} - I_o\left[\exp\left\{\frac{q}{nkT}(V + R_s I)\right\} - 1\right] - \frac{V + R_s I}{R_{\rm sh}} \tag{4}$$

where the two internal resistances R_s and $R_{\rm sh}$ can generally be neglected, and (4) is further simplified to

$$I = I_{\rm ph} - I_o\left\{\exp(AV) - 1\right\} \cong I_{\rm ph} - I_o \exp(AV) \tag{5}$$

where

$$A = \frac{q}{nkT}.$$

The parasitic resistances being neglected in (4) means that R_s is very small and $R_{\rm sh}$ is very large. For instance, R_s calculated in [19] using the MSX60's manufacturer's curve is 8 mm $\cdot\ \Omega$. Moreover, even Luque and Hegedus [18] discuss that these parasitic resistances typically associated with real solar cells are negligible. MPPT control algorithms have been studied using the formula obtained on the basis of these conditions regarding parasitic resistances (5) [9], [12]. Here, as it is impossible for users to obtain further information about A, (5) is expressed using the many properties that are listed in data sheets for solar arrays so as to easily carry out numerical analyses of $P-I$ characteristics. The short-circuit current $I_{\rm sc}$ and the open-circuit voltage $V_{\rm oc}$ are used to change (5) into

$$I_{\rm sc} = I_{\rm ph} \quad (\because V = 0,\ I = I_{\rm sc}) \tag{6}$$

$$I_o = I_{\rm sc}\exp(-AV_{\rm oc}) \quad (\because I = 0,\ V = V_{\rm oc}) \tag{7}$$

which describe two operating points in the short and open circuits. The optimum operating points ($I_{\rm pm}$, $V_{\rm pm}$) that generate the MP is expressed using (5)–(7) by

$$I_{\rm pm} = I_{\rm sc}\left[1 - \exp\left\{A(V_{\rm pm} - V_{\rm oc})\right\}\right] \tag{8}$$

$$A = \frac{1}{(V_{\rm pm} - V_{\rm oc})}\log\left(1 - \frac{I_{\rm pm}}{I_{\rm sc}}\right). \tag{9}$$

This means that (9) can convert A into a measurable quantity with the solar curve tracer. Thus, using (6) and (7), the output voltage V is given by (10) as a function of the output current I using circuit parameters $V_{\rm oc}$, $I_{\rm sc}$, $V_{\rm pm}$, and $I_{\rm pm}$. Finally, the

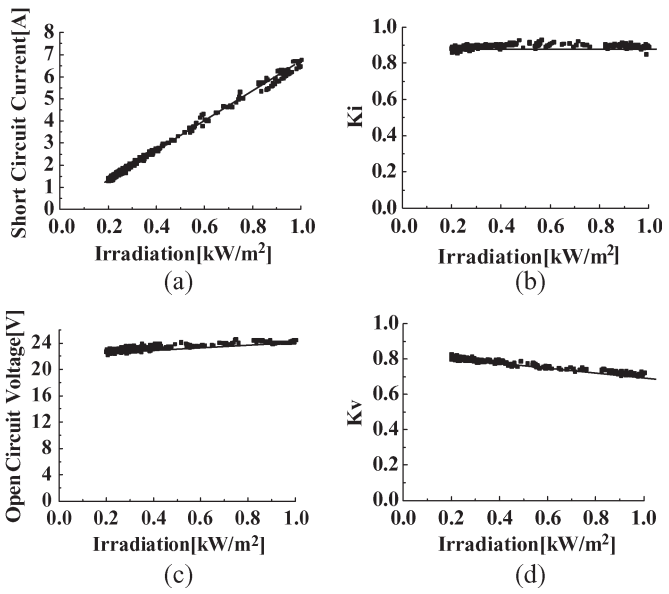

Fig. 2. Measured parameters needed for the calculation of $P-I$ characteristics when irradiation is changed. (a) $I_{\rm sc}$ characteristic. (b) k_i characteristic. (c) $V_{\rm oc}$ characteristic. (d) k_v characteristic.

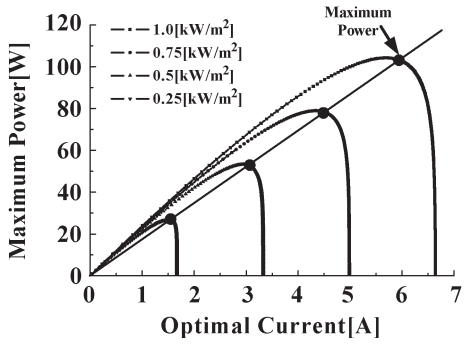

Fig. 3. Calculated $P-I$ characteristics at 25 °C.

output power P is expressed by (11) as a function of the output current I, and then $P-I$ characteristics can be calculated using (11), i.e.,

$$V = V_{\rm oc}\left\{1 + \frac{1}{A}\log\left(1 - \frac{I}{I_{\rm sc}}\right)\right\} \tag{10}$$

$$P = V \times I = I \times V_{\rm oc}\left\{1 + \frac{1}{A}\log\left(1 - \frac{I}{I_{\rm sc}}\right)\right\} \tag{11}$$

$$A = \frac{1}{(k_v - 1)}\log(1 - k_i). \tag{12}$$

Here, k_v and k_i are $V_{\rm pm}/V_{\rm oc}$ and $I_{\rm pm}/I_{\rm sc}$, respectively. These values at maximum irradiation are obtained from the data sheets for solar arrays, and the values at other irradiations are measured using the solar curve tracer. For instance, in the case of solar arrays R421-1(B) (made by Kyosera, Japan), $I_{\rm sc}$, $I_{\rm pm}$, $V_{\rm oc}$, and $V_{\rm pm}$ at rated irradiation are 6.7 A, 6 A, 24.3 V, and 18.3 V, respectively, and then these data at other irradiations are measured as shown in Fig. 2. Fig. 3 shows $P-I$ characteristics calculated using values from Fig. 2, where the temperature is kept at 25 °C. The optimal current is proportional to the MP

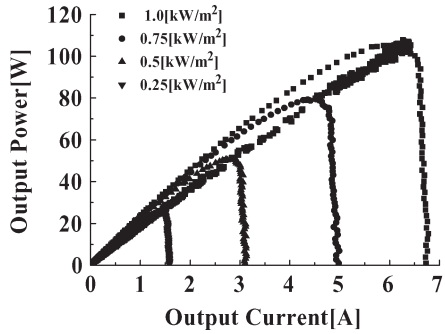

Fig. 4. Experimental verification of the linearity between MP and optimal current at 25 °C.

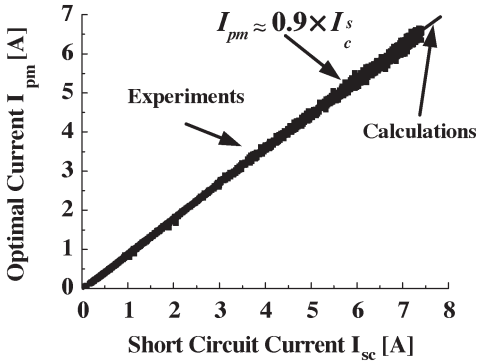

Fig. 5. Calculated relationships between the short-circuit current and the optimal current at 25 °C.

when the temperature of the solar panels is kept constant. This fact is also verified through the experimental results shown in Fig. 4. Comparison of Fig. 3 (calculated results) with Fig. 4 (experimental results), which are measured at the same temperature as the calculated results, shows that both are almost in agreement. This means that these parasitic resistances can be neglected when arguing about the linearity between the MP and the optimal current. Moreover, it is confirmed through calculational and experimental results shown in Fig. 5 that there is also a proportional relationship between the short-circuit current and the optimal current that is determined by (8).

Next, the temperature dependency of the two linear relationships obtained through the above analyses is investigated. Fig. 6 shows that the proportionality coefficient, i.e., voltage coefficient between the MP and the optimal current, remains almost constant for each temperature range when less than around half the rated optimal current, i.e., 3 A; however, the voltage coefficient gradually decreases with temperature when above half the rated value. On the other hand, Fig. 7 shows that the proportionality coefficient between the short-circuit current and the optimal current is kept constant even if the temperature is changed. This is because the short-circuit current is almost the same as the photocurrent, which relates to irradiation, and the optimal current is proportional to irradiation [13]. In addition, it is necessary to investigate the influence of shade. When solar panels are partially covered in the shade, experimental results in Fig. 8 show that although the shade has an effect on $P-V$ characteristics, there is no change in the property for which a peak appears in the $P-I$ characteristics [Fig. 8(b)]. As a result,

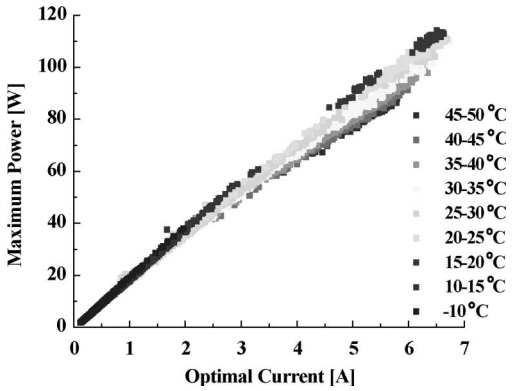

Fig. 6. Temperature dependency relationship between the optimal current and the MP.

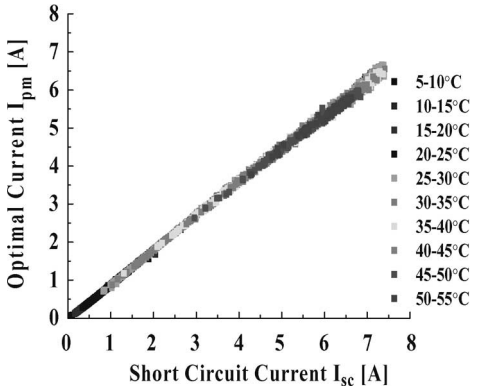

Fig. 7. Temperature dependency relationship between the short-circuit current and the optimal current.

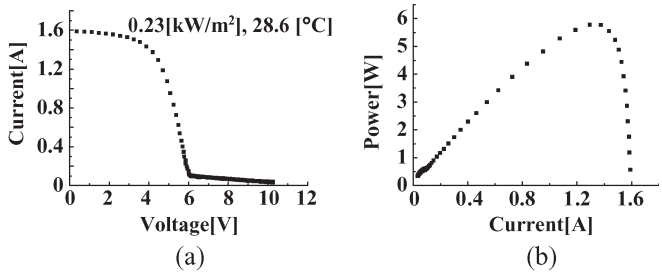

Fig. 8. Measured voltage–current and power–current characteristics. (a) Voltage versus current. (b) Current versus power.

Fig. 9 shows that the MP is mostly proportional to the optimal current even in the shade. Accordingly, it can be concluded that the facts obtained through the above verification can be used when constructing control rules for MPPT control that must be performed under various weather conditions.

B. Principal of the Proposed MPPT Control

Here, the $P-I$ characteristics are focused on, and MPPT control rules are created based on, the two facts related to the two characteristics, i.e., the MP and optimal current characteristics, and the short-circuit current and optimal current characteristics. As shown in Fig. 10, as the $P-I$ characteristics show that the output power P from the solar arrays becomes a binary function of the output current I from them, control rules to which P and I are made to correspond uniquely are required for

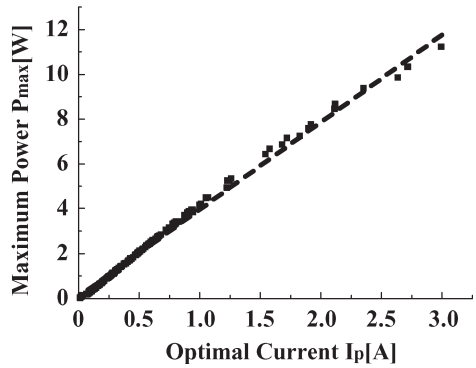

Fig. 9. Measured MP and optimal current characteristics when solar arrays are partially in the shade.

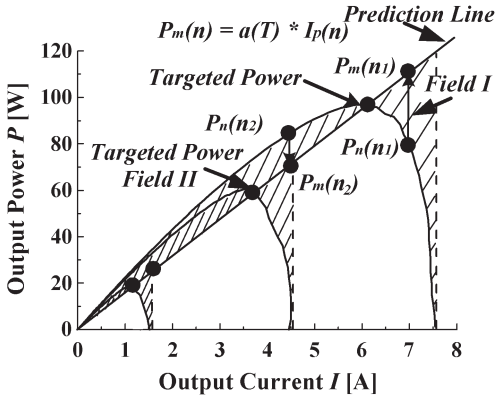

Fig. 10. Control fields for performing the MPPT control, which are divided based on a prediction line determined from the relationship between the MP and the optimal current.

MPPT control based on the $P-I$ characteristics. That is, $P-I$ characteristics are divided into two control fields, i.e., Fields I and II, based on a prediction line that associates the MP and the optimum current, as shown in Fig. 10. In this figure, "Field I" corresponds to the region where the power $P_n(n_1)$ being generated at n_1 time is lower than the power $P_m(n_1)$ on the prediction line ($P_n(n_1) < P_m(n_1)$). "Field II" is the case having the opposite relation to "Field I," i.e., $P_n(n_2) > P_m(n_2)$. Then, after judging the control field by comparison with the detected power and the power on the prediction line every sampling time, tracking procedures are needed for each judged control field in order for the output power to converge on its targeted power $P_m(n)$ of the prediction line by regulating the output current. To do so, the current reference needed to regulate the output current must be decided. That is, in "Field I," the procedure that keeps the output power on the targeted MP of the prediction line is required, which decreases the current reference. In "Field II," the reverse procedure is required. Moreover, as shown in Fig. 6, since the proportionality coefficient of the prediction line changes with temperature when the optimal current is more than half the rated one, a procedure that compensates for temperature changes is needed.

III. MPPT Control Method

Base on the MPPT control principal described in Section II, the MP P_m is controllable using the linear relationship of the

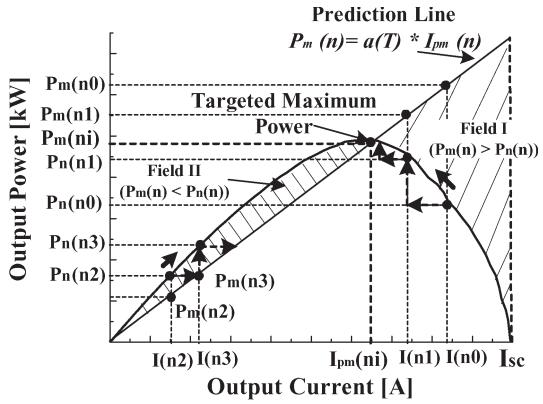

Fig. 11. Diagram for explaining the tracking processes for each control field.

MP and the optimal current $I_{\rm pm}(n)$, which is given by

$$P_m(n) = a(T) \times I_{\rm pm}(n). \tag{13}$$

Here, the proportionality coefficient $a(T)$ is a voltage factor. The parameter $a(T)$ based on Figs. 3 and 4 is given by

$$a(T) = a_0 + \Delta a(T) \tag{14}$$

where $\Delta a(T)$ is the value compensated for by temperature changes, which is determined through the hill-climbing method, and a_0 is a constant value independent of temperature, which is used when the optimal current $I_{\rm pm}(n)$ is less than half its rated value.

The MPPT control proposed here is performed so that the output power converges on the targeted power of the prediction line given by (13) while searching for the parameter $a(T)$ corresponding to the temperature of solar panels through the hill-climbing method. As shown in Fig. 11, the output current $I(n)$ of the solar arrays is regulated so that the output power $P_n(n)$ detected at the time n moves toward the suitable MP at that time, i.e., the targeted MP $P_m(n)$ on the prediction line in the control field, "Field I" or "II." As the tracking process that makes the output current $I_n(n)$ converge on the optimal operating point ($P_m(n)$, $I_{\rm pm}(n)$) differs between "Fields I" and "II," it is necessary to determine whether the operating point ($P_n(n)$, $I_n(n)$) is in "Field I" or "Field II." For that purpose, a formula that compares the output power $P_n(n)$ with the MP $P_m(n)$ that can be generated at that time is needed. The output power $P_n(n)$ can be estimated using the output current $I(n)$ and voltage $V(n)$ detected at time n from

$$P_n(n) = V(n) \times I(n). \tag{15}$$

The MP $P_m(n)$ on the prediction line that can be generated by the output current $I(n)$ at time n can be estimated based on the previously obtained prediction line given by

$$P_m(n) = a(T) \times I(n). \tag{16}$$

The two control fields are judged by comparing the power $P_m(n)$ estimated from (17) with the power $P_n(n)$ currently being generated in the solar arrays. In other words, it is judged that in cases where $P_n(n)$ is less than $P_m(n)$, the operating point on the $P-I$ curve lies in "Field I," whereas in the opposite cases, it lies in "Field II."

Next, procedures to determine the current reference, which need to perform the proposed MPPT control for each control field, are studied.

A. Procedures to Determine the Current Reference in Field I

By comparing $P_n(n)$ with $P_m(n)$, when the operating point is judged to be in "Field I," the following procedure is executed: The current reference $I_{\rm pr}(n+1)$ for the output current $I(n+1)$ that should flow at the next time $(n+1)$ must be predetermined so as to reach the MP targeted on the prediction line while making the detected output current $I(n)$ decrease by $\Delta I(n)$. Thus, it is necessary to determine the maximum amount that can make the current decrease, i.e.,

$$I_{\rm pr}(n+1) = I(n) - \Delta I(n). \tag{17}$$

In "Field I," as the controllable range of the output current is between the short-circuit current $I_{\rm sc}(n)$ and the optimal current $I_{\rm pm}(n)$, it is given by the inequality

$$I_{\rm pm}(n) \le I(n) \le I_{\rm sc}(n). \tag{18}$$

On the other hand, as shown by Fig. 5, $I_{\rm pm}(n)$ is proportional to $I_{\rm sc}(n)$. Then, expressing the proportionality factor using $k_{\rm sc}$, $I_{\rm pm}(n)$ is given by

$$I_{\rm pm}(n) = k_{\rm sc} \times I_{\rm sc}(n). \tag{19}$$

Here, $k_{\rm sc}$ is $(I_p)_{\rm rated}/I_{\rm sc}$, which is the ratio of the short-circuit current and the rated optimum current at the time of factory shipment or applications. It is set up as a default value in controllers. In the case of Fig. 5, $k_{\rm sc}$ is 0.9. Normally, it exists between 0.9 and 0.95. The set default value is periodically updated using the corrected ratio $I_p/I_{\rm sh}$, i.e., the ratio of the short-circuit current and optimal current that have been measured. In this case, the short-circuit current can be easily measured by controlling a power switch device added to the output side of the solar arrays [14].

Thus, the decreasing rate $\Delta I(n)$ of the current reference is given by

$$\Delta I(n) < (\Delta I(n))_{\max} \left(= I_{\rm sc}(n) - I_{\rm pm}(n)\right). \tag{20}$$

If (19) is substituted for (20), $\Delta I(n)$ can be obtained as

$$\Delta I(n) < (1 - k_{\rm sc}) \times I_{\rm sc}(n). \tag{21}$$

Therefore, as $\Delta I(n)$ should be less than the value of the right term in (21), $(1-k_{\rm sc}) \times I(n) (< (1-k_{\rm sc}) \times I_{\rm sc}(n))$ is applied as the value of $\Delta I(n)$, which satisfies (21). As a result, the optimal current reference $I_{\rm pr}(n+1)$ for the output current $I(n+1)$ that should flow at the next time $(n+1)$ is given by

$$I_{\rm pr}(n+1) = I(n) - \Delta I(n) = k_{\rm sc} \times I(n) \tag{22}$$

as the control rule by which the output current $I(n)$ at time n arrives at the optimal current $I_{\rm pm}(n)$ on the prediction line of

Fig. 11. This procedure enables the output current to arrive at the maximum point within the minimum time as the optimal current reference $I_{\rm pr}(n+1)$ is predetermined based on (22) using the largest possible decreasing rate $\Delta I(n)$. The right term in (22) is eventually expressed only with the output current $I(n)$ detected at time n. Here, the precision of the maximum output power obtained through this procedure can be controlled by changing $k_{\rm sc}$ in (22) between $(I_p)_{\rm rated}/I_{\rm sc}$ and 1.

Next, the tracking algorithm cited above is concretely explained by examples with numbers obtained based on Fig. 10, which are the theoretical targeted point $(P_m(n), I_{\rm pm}(n))$, initial $a(T)$, and $I_p/I_{\rm sc}$ given by (96 W, 6.0 A), 16.0, and 0.9, respectively.

First, the voltage and current that were measured at time $n1$ are 11.3 V and 7 A, respectively. In this case, the generated power $P_n(n1)$ on the $P-V$ characteristic of Fig. 10 and the power $P_m(n1)$ on the prediction line is 79.1 W$(=11.3\ {\rm V}\times 7\ {\rm A})$ and 112 W$(=16.0\times 7\ {\rm A})$, respectively. Then, calculating the power difference $\Delta P(n1)(=P_m(n1)-P_n(n1))$, since the sign of this value is judged to be positive $(\because\ 112\ {\rm W}-79.1\ {\rm W}>0)$, the MPPT control in "Field I" is performed (Here, as long as this sign is positive, the generated power always lies in "Field I".) Second, the reference $I_{\rm pr}(n2)$ for the current that should flow at the next time (sampling time) $n2$ is predetermined based on (22). In this case, it is 6.3 A$(=0.9\times 7\ {\rm A})$. Here, before setting the predetermined 6.3 A to the actual current reference, it is confirmed that the output power generated at the next time $n2$ can still remain in "Field I" even if the output current is controlled at 6.3 A. That is, the power $P_m(n2)$ appearing on the prediction line at the next time $n2$ is previously checked whether it exceeds the currently generated power because it is supposed that the generated power may enter into "Field II" if not so. As $P_m(n2)$ is 100.8 W$(=16\times 6.3\ {\rm A})(>79.1\ {\rm W})$, this requirement is satisfied. Thus, 6.3 A is finally adopted as the actual current reference $I_{\rm pr}(n2)$. Then, the current regulator is operated so that the output current accords with the current reference $I_{\rm pr}(n2)(=6.3\ {\rm A})$ predetermined at time $n1$ until the next time $n2$. Then, at time $n2$, the generated voltage and output current are detected as 15 V and 6.3 A, respectively. In this case, the generated power $P_n(n2)$ is obtained as 94.5 W$(=15\ {\rm V}\times 6.3\ {\rm A})$. These series procedures are repeatedly done until it is confirmed that the power generated at the next sampling time might go into "Field II." The time until this situation appears can be explained as follows: At time $n2$, moreover, the current reference $I_{\rm pr}(n3)$ that should flow at time $n3$ is predetermined as 5.7 A$(=6.3\ {\rm A}\times 0.9)$. In this case, as $P_m(n3)$ is obtained as 91.2 W$(=16\times 5.7\ {\rm A})$, this cannot satisfy the above requirement $(\because P_n(n2)(=94.5\ {\rm W})>P_m(n3)(=91.2\ {\rm W}))$. If the output current is kept controlled by $I_{\rm pr}(n3)$, the power generated at time $n3$ will go into "Field II." Thus, the MPPT control performed in "Field I" is stopp ed at that time. As a result, 94.5 W is judged as the MP obtained in the field.

B. Procedures to Determine the Current Reference in Field II

Fig. 11 shows the region where the output power arrives at its maximum by increasing the output current $I(n)$ until it becomes the optimal current $I_{\rm pm}(n)$ on the prediction line of Fig. 11. If the output current $I(n)$ at time n agrees with the optimal current $I_{\rm pm}(n)$, the maximum output power $P_m(n)$ on the prediction line is given by (16). However, in this case, as shown by Fig. 11, when the actual operating points on the $P-I$ curve, for instance, $(I(n2),\ P(n2))$ and $(I(n3),\ P(n3))$, exist in "Field II," the power $P_m(n)$ on the prediction line at these times is smaller than the generated output power $P(n)$ until $P(n)$ accords with the true targeted MP. That is

$$P_n(n)\geq P_m(n) \tag{23}$$

is satisfied in "Field II." Accordingly, the true targeted MP should be larger than $P_m(n)$. So, the optimal current reference $I_{\rm pr}(n+1)$ at the next time $(n+1)$ is increased by

$$I_{\rm pr}(n+1)=P_n(n)/a(T) \tag{24}$$

so that the output current $I(n)$ can arrive at the point where error $\Delta\varepsilon$, i.e., ratio of the power difference $\Delta P(n)(=P_n(n)-P_m(n))$, and the rated MP $(P_{\rm max})_{\rm rated}$ become less than the given error. This procedure is repeated until the above error $\Delta\varepsilon$ reduces to the predetermined value. In this process, as the optimal current reference is determined by the shortest possible distance between the operating point and the prediction line, the output current can arrive at the MP within the minimum time.

Based on the current reference determined for each control field, $P_n(n)$ detected at time n converges on the MP $P_m(n)$ that can be generated at that time as shown in Fig. 11.

Next, the tracking algorithm cited above is explained based on numbers obtained from Fig. 10 under the same conditions as in Section III-A. As long as the output current is controlled by the current reference $I_{\rm pr}(n+1)$ at the next time $(n+1)$, which is predetermined based on (24), the power generated at the next time $(n+1)$ does not go into "Field I." Then, the MPPT control performed in "Field II" is stopped only when it was judged that the power difference $\Delta P(n)(=(P_n(n)-P_m(n))/(P_{\rm max})_{\rm rated})$ becomes less than the given error $\Delta\varepsilon$. Here, $(P_{\rm max})_{\rm rated}$ and $\Delta\varepsilon$ are set to 96 W and 1%, respectively.

First, the voltage and the current (in Fig. 10), which were measured at time $n1'$, are 19.3 V and 4.1 A, respectively. In this case, $P_n(n1')$ and $P_m(n1')$ are obtained as 79.1 W$(=19.3\ {\rm V}\times 4.1\ {\rm A})$ and 65.6 W$(=16\times 4.1\ {\rm A})$, respectively. Here, since $P_n(n1')$ $(=79.1\ {\rm W})$ is larger than $P_m(n1')$ $(=65.6\ {\rm W})$, the MPPT control in "Field II" is performed. Then, the current reference $I_{\rm pr}(n2')$ at the next time $n2'$ is predetermined using (24) as 4.9 A$(=79.1\ {\rm W}/16.0)$. As the output current is controlled by the current reference of 4.9 A, the actual output current and voltage are detected as 4.9 A and 18.6 V, respectively, and then the generated powers $P_n(n2')$ and $P_m(n2')$ at $n2'$ are obtained as 91.1 W$(=4.9\ {\rm A}\times 18.6\ {\rm V})$ and 78.4 W$(=16\times 4.9\ {\rm A})$. In this case, $\Delta\varepsilon$ is 13.2% $(=((91.1\ {\rm W}-78.4\ {\rm W})/96\ {\rm W})\times 100\%)$. Thus, the MPP control is kept on. Then, the current reference $I_{\rm pr}(n3')$ at the next time $n3'$ is predetermined as 5.7 A$(=91.1\ {\rm W}/16.0)$. As a result, since the

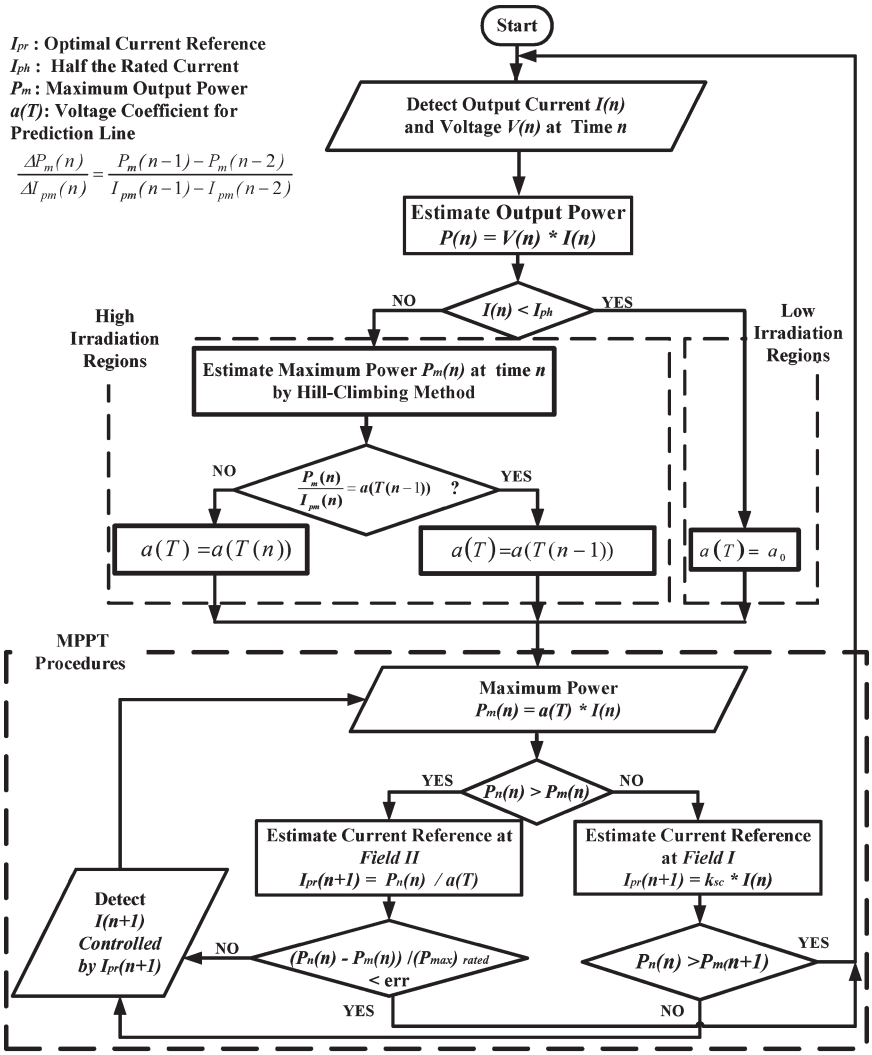

Fig. 12. Flowchart for the proposed MPPT control method.

actual output current 5.7 A and voltage 16.7 V are detected, $P_n(n3')$ and $P_m(n3')$ are estimated as 95.8 W($= 5.7$ A $\times$ 16.8 V) and 91.2 W($= 16 \times 5.7$ A), respectively. In this case, $\Delta\varepsilon$ is 4.8% ($= ((95.8\text{ W} - 91.2\text{ W})/96\text{ W}) \times 100\%$). Moreover, MPPT control is performed, and then $I_{\rm pr}(n4')$ is predetermined as 5.99 A($= 95.8$ W$/16$) at the next time $n4'$. In this case, the actual current and voltage are detected as 5.99 A and 16.02 V, respectively. Then, $P_n(n4')$ and $P_m(n4')$ are estimated as 96.0 W($= 5.99$ A $\times$ 16.02 V) and 95.8 W($=$ 16×5.99 A). As a result, since $\Delta\varepsilon$ becomes less than 1%, MPPT control is stopped, and then the MP obtained from "Field II" is judged as 96 W.

C. Algorithm for Performing the Proposed MPPT Control Method

The control procedure cited above is summarized in the flow chart shown in Fig. 12. First, the output power $P(n)$ generated from the solar arrays is estimated by detecting the output current $I(n)$ and voltage $V(n)$ of the solar arrays. Next, the detected output current $I(n)$ is compared with the value $I_{\rm ph}$ at half the rated current that corresponds to the mean value of irradiation obtained at the time of fine controlling fields, i.e., when "Fields I" and "II" are judged. In cases where the detected output current $I(n)$ is less than the predetermined $I_{\rm ph}$, the voltage coefficient $a(T)$ of the prediction line is assumed to be kept almost at a_0, which has already been estimated through the hill-climbing method when the output current $I(n)$ is around $I_{\rm ph}$. Using the already obtained a_0, MPPT control is performed based on the prediction control method cited above, which makes the output power $P(n)$ move toward the maximum output power $P_m(n)$, dividing $P{-}I$ curves into "Fields I" and "II." When the detected output current $I(n)$ is more than $I_{\rm ph}$, only $\Delta a(T)$ is estimated based on the differential $\Delta P_m(n)/\Delta I_{\rm pm}(n)$ $(= (P_m(n-1) - P_m(n-2))/(I_{\rm pm}(n-1) - I_{\rm pm}(n-2)))$, which is the ratio of the difference regarding the MP and the optimal current already obtained at times $(n-1)$ and $(n-2)$ because the voltage coefficient $a(T)$ may vary with the temperature of the solar arrays. Temperature changes occur more slowly than the speed that identifies the parameter. Thus, $a(T(n))$ obtained at time n is adopted as the parameter produced by change of temperature only when the value $a(T(n))$ differs from $a(T(n-1))$ already obtained at time $(n-1)$.

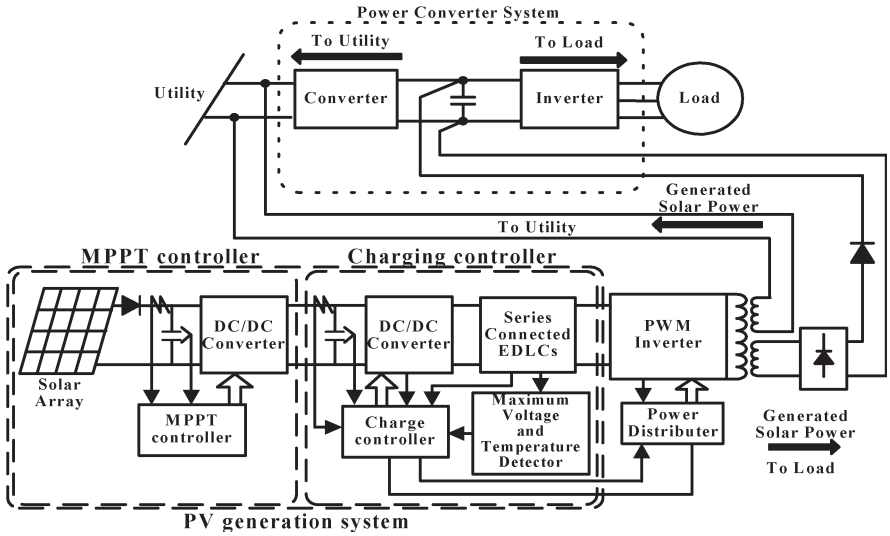

Fig. 13. PV generation systems including the proposed MPPT control method.

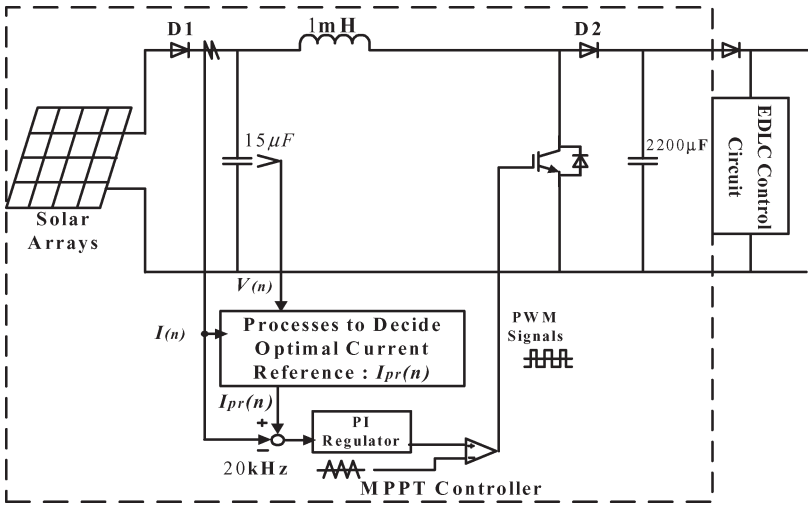

Fig. 14. Block diagram of MPPT controller shown in Fig. 13.

IV. Experimental Verification of the Proposed MPPT Control Method

A. PV Generation System for Verifying the Proposed MPPT Control

Fig. 13 shows a schematic diagram of the PV system, which makes it possible to supply electric power generated by solar arrays to the utility or load [20]. In order to acquire the generated energy efficiently through MPPT control, this system has a charging controller that is composed of a number of ultra-electric double-layer capacitors (ultra-EDLCs) connected in series. As shown in Fig. 14, the MPPT controller in Fig. 13 consists of a microcomputer performing the control flow of Fig. 12 using DSP and the first dc/dc converter formed by the boost type chopper that is driven based on pulsewidth modulation (PWM) signals generated from the microcomputer so that solar arrays can generate the MP at that time. The second dc/dc converter regulates the voltage output from the first dc/dc converter so as not to exceed the isolation voltage of all the series-connected ultra-EDLCs. In addition, charging control for series-connected EDLCs is performed while supervising the maximum voltage and allowable temperature of each EDLC so that the power corresponding to the instantaneous power generated from solar arrays can flow into the EDLCs. The charged solar power is directly regenerated to the utility through the PWM inverter, and it is supplied to the load or utility through the dc intermediate circuit of the power converter system composed of a converter (rectifier) and an inverter. Experiments are done using the PV generation system. Only results required to verify the proposed MPPT control are shown below.

B. Generated Power Acquisition Performance of the Proposed MPPT Control Method

The proposed MPPT control method is characterized by improving the acquired response characteristics of the generated power at low irradiations. Thus, first, the response characteristics until the generated power arrives at the targeted MP are investigated at low irradiation. As shown in Fig. 15(a), the targeted generation power that evaluates the response

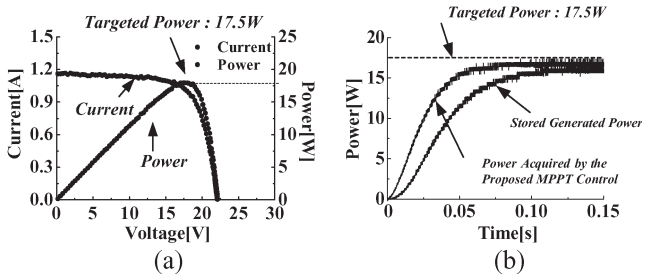

Fig. 15. Response performance of the proposed MPPT method at low irradiation. (a) Targeted power measured at low irradiation 0.15 kW/m^2. (b) Response characteristics at the targeted power: 17.5 W.

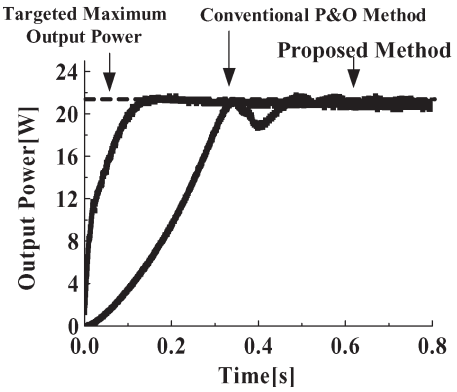

Fig. 16. Comparison of stability and accuracy between conventional P&O and proposed methods.

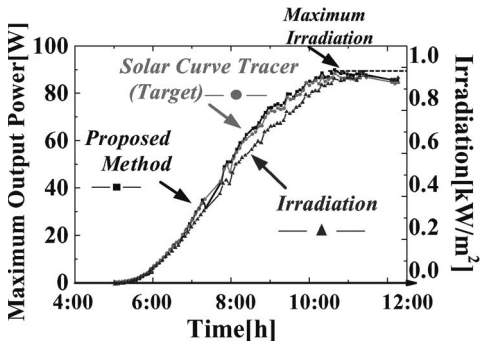

Fig. 17. MP generation characteristics until the maximum irradiation in the day when the proposed MPPT method is used.

characteristics of the acquired power is measured using the solar curve tracer ("EKO-123, Japan") when the irradiation is 15% of the rated one. Fig. 15(b) shows that the generated power quickly responds with the time constant of around 30 ms until reaching the targeted MP of 17.5 W. The conventional P&O method has a stability problem at low irradiation. Thus, another effect of the proposed method on the stability and accuracy to acquire the MP is verified. Fig. 16 shows that the MP can be stably and precisely controlled in comparison with the conventional P&O method even at low irradiation. The conventional P&O method is the technique to make the generated power converge on an MP point in $P-V$ or $P-I$ characteristics while straddling the MP point according to the sign of dP/dV or dP/dI, i.e., while swinging between "Field I" and "II," which are discussed in this paper. Thus, as shown in Fig. 16, it turns out from the experimental result obtained using the conventional P&O method that the generated power certainly reaches a targeted value while causing hunting (oscillation). Moreover, even after the generated power arrives near a target value, oscillations continue without stopping although their width becomes small. If the generated power with hunting components is supplied to the utility, various kinds of bad effects such as power loss and noises may be given not only on the utility sides but also on the load sides via power source lines. The MPPT control discussed here is proposed in order to solve this problem. The experimental result shows that the generated power quickly responds to the targeted MP without any hunching phenomenon, and it is kept at the targeted MP without any swing phenomenon even after reaching the target value. This is because the proposed MPPT control is performed so that the generated power approaches its target only from the judged "Field" after the generated power is judged whether it lies in "Field I" or "II." Therefore, the proposed MPPT controller has the ability to quickly acquire the MP without any hunting phenomenon. As a result, by paying attention to the MP generation characteristics, it is confirmed from Fig. 17 that the maximum generation power can be obtained over all types of irra diations in accordance with the targeted MP obtained through the solar curve tracer.

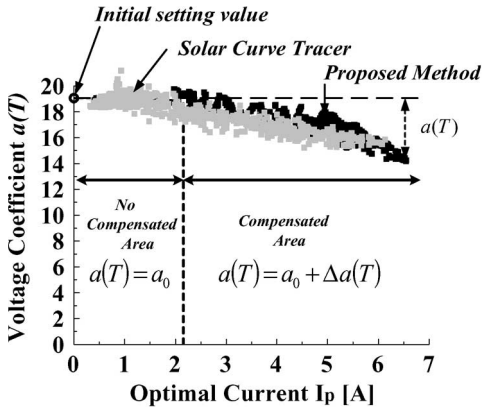

Fig. 18. Verification of the voltage coefficient identification performance of the proposed method using the solar curve tracer.

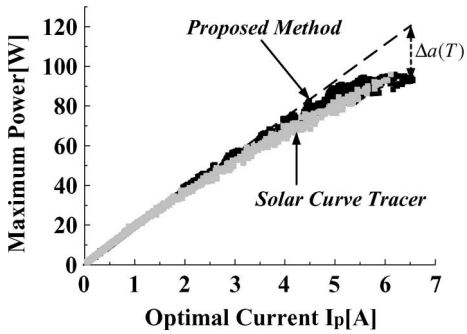

Fig. 19. Verification of the proposed MPPT method to control relationships between the optimal current and MP using the solar curve tracer (temperature range: 10 °C–55 °C).

C. Verification of Temperature Compensation Function of the Voltage Coefficient

In order to check whether the proposed MPPT method has the ability to control the MP output over a wide range of optimal

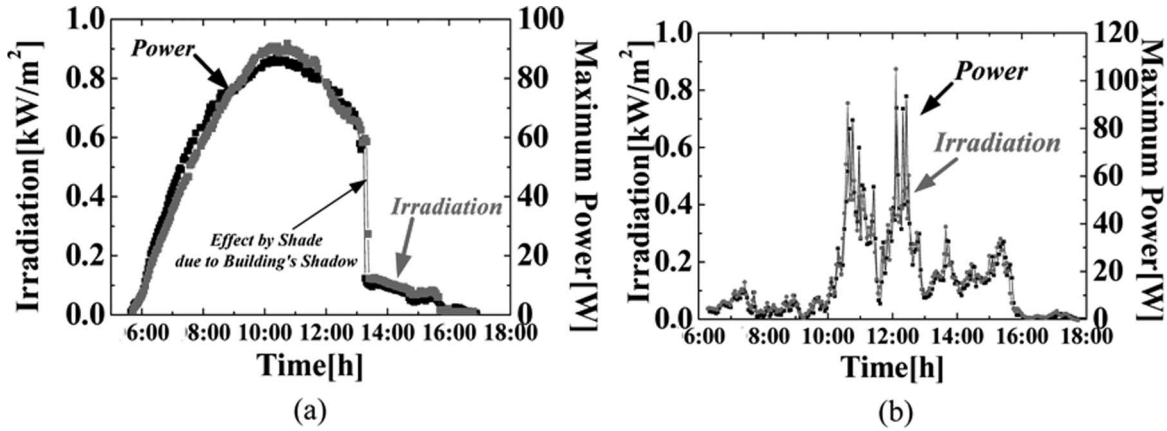

Fig. 20. Acquired MP characteristics of the proposed MPPT control method when the weather changes. (a) When the weather is fine. (b) When the weather changes frequently.

currents corresponding to weather conditions, it is necessary to examine whether the voltage coefficient is properly identified. In this paper, the effectiveness of the procedures to estimate the voltage coefficient is verified using the solar curve tracer, which is a good measurement tool for evaluating the performance of PV generation systems. In the compensated area where the optimal current is more than half the rated one, the influence of temperature variations has an effect on the voltage coefficient. Fig. 18 shows that the voltage coefficient is properly estimated in comparison with references obtained from the solar curve tracer. As a result, as shown in Fig. 19, the MP and optimal current characteristics are obtained, corresponding to actual systems in which the temperature changes.

D. MP Acquisition Effect Under Various Weather Conditions

Finally, the generation performance of the proposed MPPT method under various weather conditions is checked. Fig. 20(a) shows the MP generation property acquired through MPPT control when the solar panels are suddenly covered by shade due to a building's shadow on a fine day. It is confirmed that the MP can be acquired corresponding to changing irradiations. Fig. 20(b) shows that the MP can also be acquired even if the weather is frequently changed.

V. Conclusion

An MPPT control method indispensable to PV generation systems, which has the ability to generate maximum output power even if weather conditions are changed, was studied in this paper. In the proposed MPPT control method, the optimal current reference needed to converge the output current on the optimal operation point of the prediction line was determined by dividing $P-I$ characteristics into two control fields using two properties, i.e., linear relationships satisfied between the MP and the optimal current, and the short-circuit current and the optimal current. In this case, the voltage coefficient (proportionality coefficient) of the prediction line at large irradiation (optimal current) was identified using the hill-climbing method in order to compensate for the temperature changes of solar panels. The effectiveness of the proposed method was verified through experiments under various weather conditions.

References

[1] D. Snowdon, "Hardware and software infrastructure for the optimization of Sunswift II," B.E. thesis, School Electr. Eng. Telecommun. and School Comput. Sci. Eng., Univ. New South Wales, Kensington, Australia, Nov. 2002.

[2] S. Chin, Gadoson, K. Nordstrom "NERD GIRLS Maximum Power Point Tracker," *Tufts University Senior Design Project*, Dept. Elect. Eng. Comput. Sci., Tufts Univ., Boston, MA, 2003.

[3] *The Bit Bucket Maximum Power Point Trackers*. [Online]. Available: http://www.drgw.net/workshop/MPPT/mppt.html

[4] *Project-System Regarding MPPTs.* [Online]. Available: http://www.sungroper.asn.au/project/ *MPPTs: Contents Regarding Beil.* [Online]. Available: http://www.sungroper.asn.au/project/mppts.html#Beil

[5] T. Ouchi, H. Fujikawa, S. Masukawa, and S. Iida, "A control scheme for three-phase current source inverter in interactive photovoltaic system," *Trans. Inst. Electr. Eng. Jpn.*, vol. 120-D, no. 2, pp. 230–238, Feb. 2000.

[6] T. Kitano, M. Matsui, and D. Xu, "A maximum power point tracking control scheme for PV system based on power equilibrium and its system design," *Trans. Inst. Electr. Eng. Jpn.*, vol. 121-D, no. 12, pp. 1263–1269, 2001.

[7] H. Dong, H. Sugimoto, and N. Nishio, "A maximum power tracking control method for photovoltaic power generation system based on derivation of output power with respect to output voltage," *Trans. Inst. Electr. Eng. Jpn.*, vol. 118-D, no. 12, pp. 1435–1442, 1998.

[8] T. Kitano, M. Matsui, and D. Xu, "A MPPT control scheme for PV system utility limit cycle operation and its system design," *Trans. Inst. Electr. Eng. Jpn.*, vol. 122-D, no. 4, pp. 382–389, 2002.

[9] Y.-C. Kuo, T.-J. Liang, and J.-F. Chen, "Novel maximum-power-point-tracking controller for photovoltaic energy conversion system," *IEEE Trans. Ind. Electron.*, vol. 48, no. 3, pp. 594–601, Jun. 2001.

[10] T.-F. Wu, C.-H. Chang, and Y.-K. Chen, "A fuzzy-logic-controlled single-stage converter for PV-powered lighting systems applications," *IEEE Trans. Ind. Electron.*, vol. 47, no. 2, pp. 287–296, Apr. 2000.

[11] M. Veer char, T. Sanyo, and K. Legato, "Neural-network-based maximum-power point tracking of coupled-inductor interleaved-boost-converter-supplied PV system using fuzzy controller," *IEEE Trans. Ind. Electron.*, vol. 50, no. 4, pp. 749–758, Aug. 2003.

[12] C. Hua, J. Lin, and C. Shen, "Implementation of a DSP-controlled photovoltaic system with peak power tracking," *IEEE Trans. Ind. Electron.*, vol. 45, no. 1, pp. 99–107, Feb. 1998.

[13] J. H. R. Enslin, M. S. Wolf, D. B. Snyman, and W. Swiegers, "Integrated photovoltaic maximum power point tracking converter," *IEEE Trans. Ind. Electron.*, vol. 44, no. 6, pp. 769–773, Dec. 1997.

[14] T. Noguchi, S. Togashi, and R. Nakamoto, "Short-current pulse-based maximum-power-point tracking method for multiple photovoltaic-and-converter module system," *IEEE Trans. Ind. Electron.*, vol. 49, no. 1, pp. 217–223, Feb. 2002.

[15] C.-T. Pan, J.-Y. Chen, C.-P. Chu, and Y.-S. Huang, "A fast maximum power point tracker for photovoltaic power systems," in *Proc. IEEE IECON*, San Jose, CA, vol. 1, pp. 390–393.

[16] N. Mutoh, T. Matuo, K. Okada, and M. Sakai, "Prediction-data-based maximum-power-point-tracking method for photovoltaic power generation systems," in *Proc. IEEE PESC*, Cairns, Australia, Jun. 2002, vol. 3, pp. 1489–1494.

[17] N. Mutoh, M. Ohno, and T. Inoue, "A method to perform a MPPT control while searching parameters corresponding to weather condition for PV generation systems," in *Proc. IEEE IECON*, Busan, Korea, Nov. 2004, CD-ROM.
[18] A. Luque and S. Hegedus, *Handbook of Photovoltaic Science and Engineering*. Hoboken, NJ: Wiley, 2002, pp. 87–111.
[19] G. Walker, "Evaluating MPPT converter topologies using a MATLAB PV model," *J. Electr. Electron. Eng.*, vol. 21, no. 1, pp. 49–56, 2001.
[20] N. Mutoh and T. Inoue, "A controlling method for charging photovoltaic generation power obtained by a MPP control method to series connected ultra-electric double layer capacitors," in *Proc. IEEE-IAS Annu. Meeting*, Seattle, WA, Oct. 3–7, 2004, CD-ROM.

Nobuyoshi Mutoh (M'89–SM'92) was born in Chiba, Japan, in 1948. He recieved the Ph.D. degree in engineering from Waseda University, Tokyo, Japan, in 1991. He completed the first half of his Ph.D. degree in the Science and Engineering Research Division, Graduate School, Waseda University, in March 1975.

In April 1975, he joined the Hitachi Research Laboratory, Hitachi, Ltd. From February 1995 to February 1998, he was a Senior Engineer in the Elevator Development Center, Mito Works of Hitachi, Ltd. From February 1998 to March 2000, he was a Senior Researcher in the Second Department of Power Electronics Research, Hitachi Research Laboratory. He became a Professor in the Department of Electronic Systems Engineering, Tokyo Metropolitan Institute of Technology in April 2000. He is currently a Professor with the Department of Systems Design, Graduate School, Tokyo Metropolitan University, Tokyo, Japan. His research fields are ECO vehicle intelligent control systems, renewable energy and distributed power generation systems such as photovoltaic, wind power, and fuel-cell control systems, and electromagnetic compatibility control techniques regarding power electronics.

Dr. Mutoh is an Associate Editor of the IEEE TRANSACTIONS ON INDUSTRIAL ELECTRONICS. He is a Registered Professional Engineer. He received an OHM Technology Award in 1989, a Kanto District Invention Award in 1994, and several other distinguished industrial awards in Japan.

Masahiro Ohno was born in 1982. He received the B.S. degree in 2004 from the Department of Electronic Systems Engineering, Tokyo Metropolitan Institute of Technology, Tokyo, Japan, where he is currently working toward the M.S. degree in the Department of Intelligent Systems.

His area of research is photovoltaic generation systems.

Takayoshi Inoue received the degree from the Department of Electronic Systems Engineering, Tokyo Metropolitan Institute of Technology, Tokyo, Japan, in 2003, and the M.S. degree from the Department of Intelligent Systems, Tokyo Metropolitan Institute of Technology, in 2004.

He is currently with Meidensha Corporation, Tokyo. His area of research is photovoltaic generation systems.